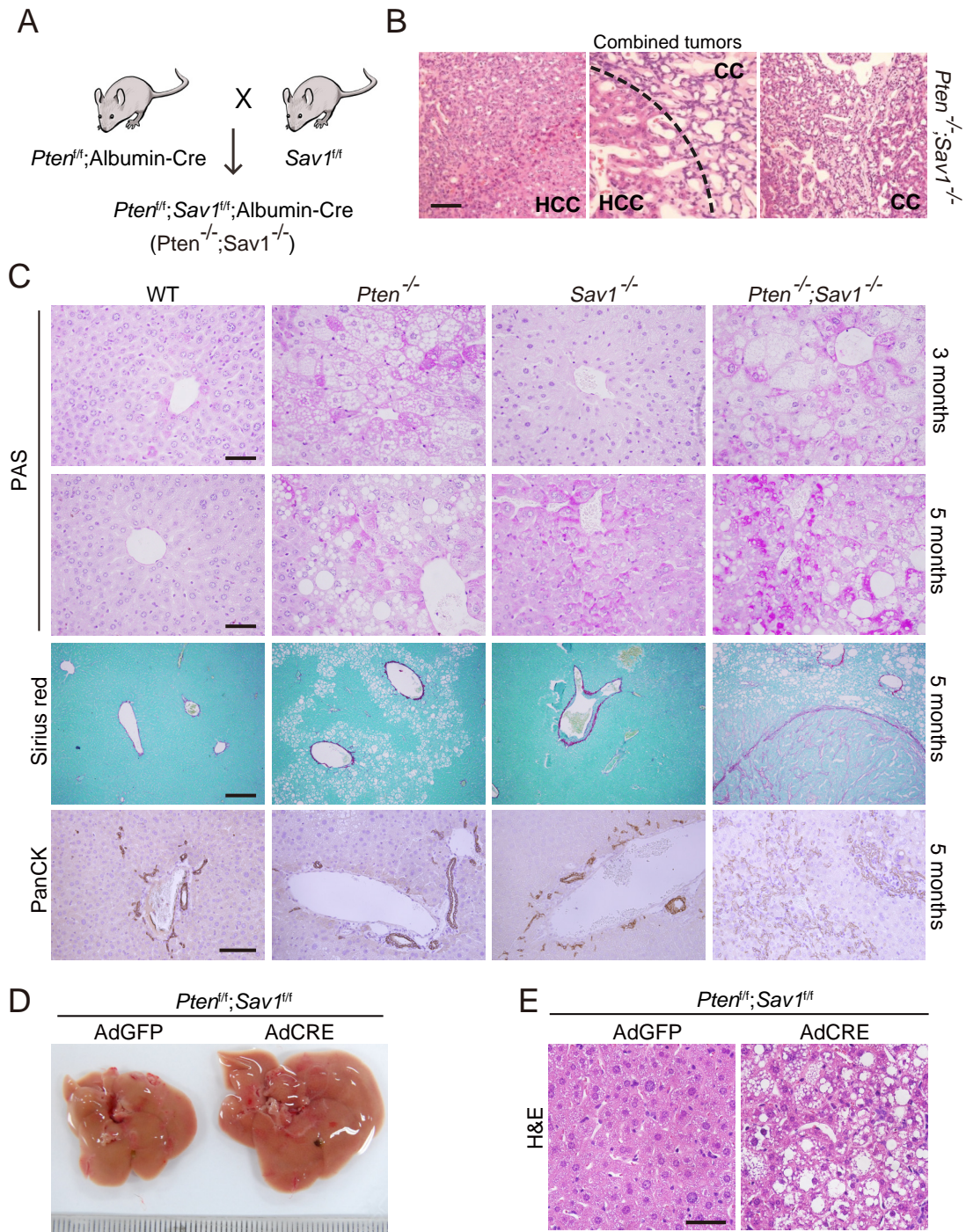
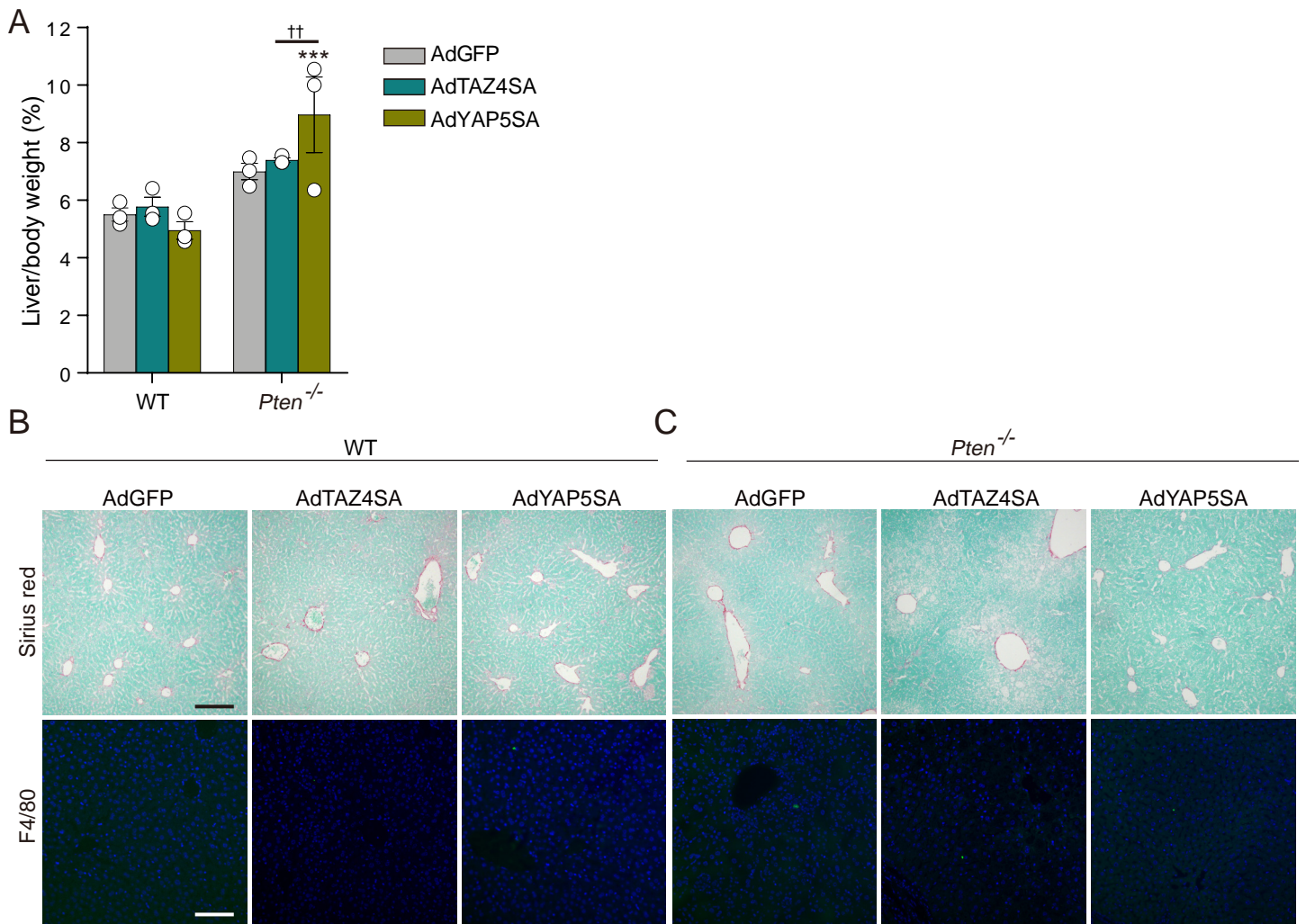


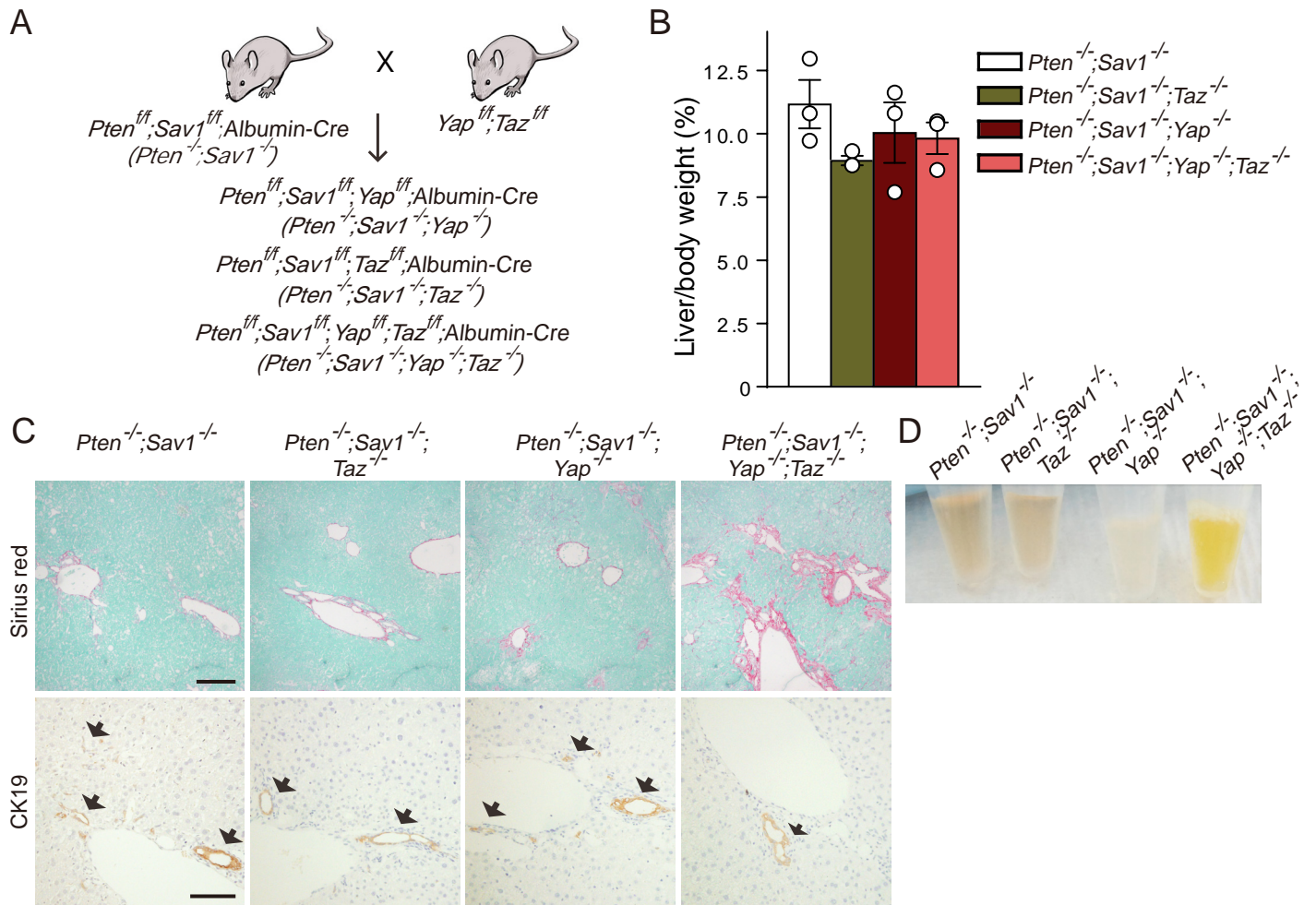
SUPPLEMENTAL DATA



Supplemental Figure 1. Liver-specific *Pten* and *Sav1* double-knockout (DKO) mice show accelerated development of liver dysfunction. (A) Schematic for the generation of liver-specific DKO mice. (B) Representative H&E staining of combined hepatocellular carcinoma (HCC) and cholangiocarcinoma (CC) tumor types in DKO mouse livers. Scale bar, 100 μ m. (C) PAS, Sirius red, and panCK immunohistochemical staining of the livers of mice at the indicated ages. Scale bars: 50 μ m (PAS), 200 μ m (Sirius red), and 100 μ m (panCK). $n = 5$ for each group in all analyses. (D-E) Acute adult-stage deletion of *Pten* and *Sav1* induces fatty liver. Microscopic appearance (D) and H&E staining (E) of livers from 6-week-old *Pten^{fl/fl};Sav1^{fl/fl}* mice injected with adenovirus encoding CRE and GFP (control). Scale bars, 50 μ m.

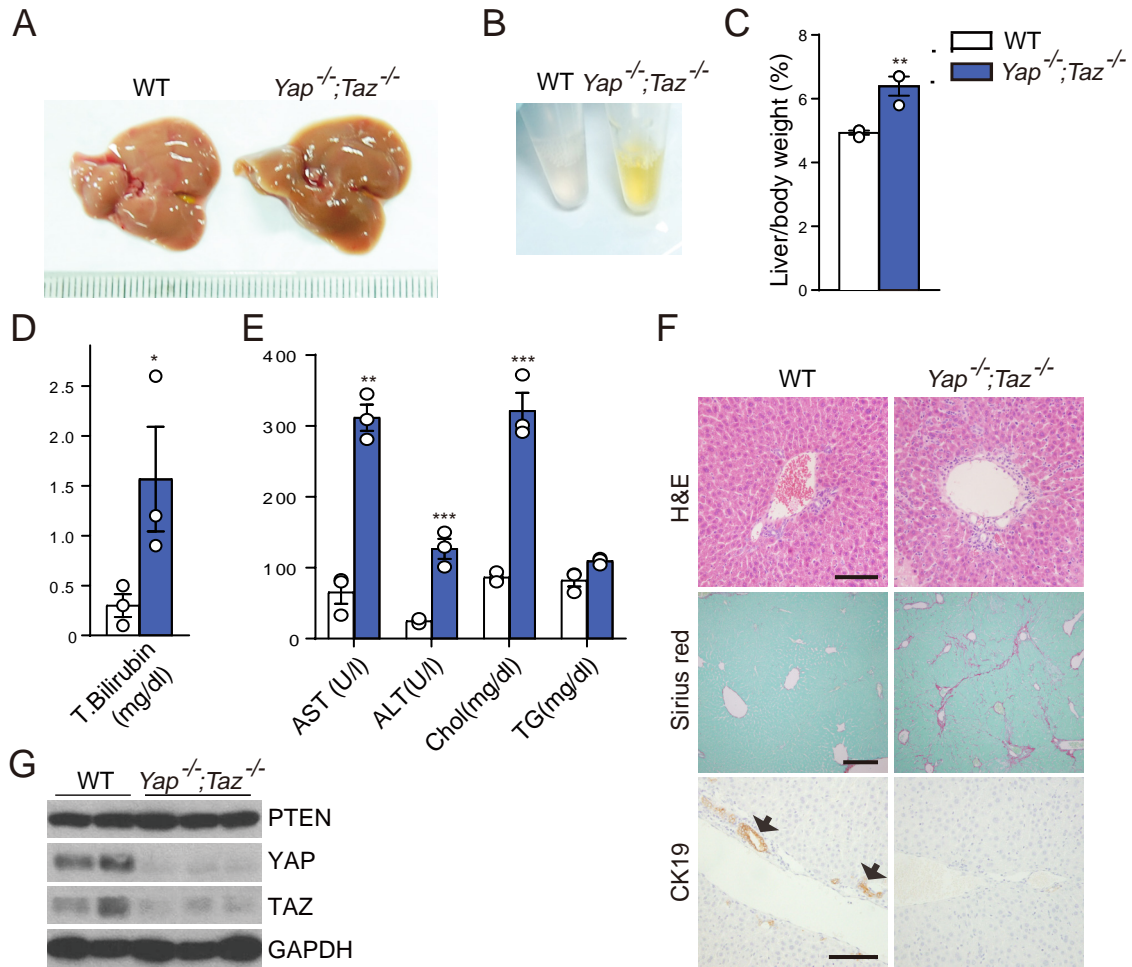


Supplemental Figure 2. A short-term increase of YAP or TAZ activity promotes fatty liver development without fibrosis or inflammation. The liver-to-body weight ratio (**A**) as well as representative Sirius red staining and F4/80 immunofluorescence staining (green fluorescence) of the liver (**B, C**) are shown for 6-week-old WT (**B**) or *Pten*^{-/-} (**C**) mice (n = 3) 4 days after injection with adenoviruses encoding GFP, TAZ4SA, or YAP5SA. Nuclei in (**B**) and (**C**) were stained with 4',6-diamidino-2-phenylindole (blue fluorescence). Scale bars, 200 μ m (top panels) or 100 μ m (bottom panels). Quantitative data are means \pm s.e.m. *** P < 0.001 versus the corresponding value for AdGFP, †† P < 0.01 for the indicated comparison (one-way ANOVA).

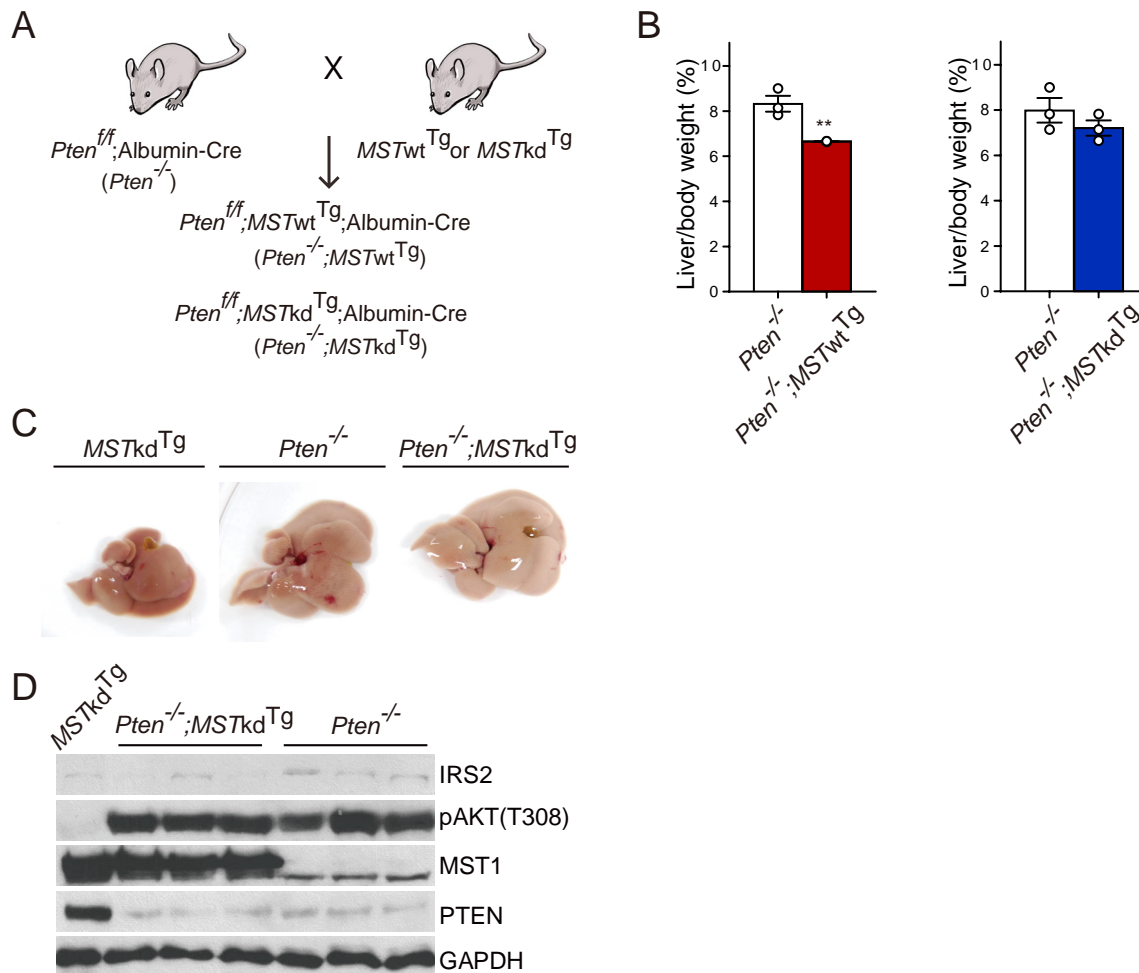


Supplemental Figure 3. $Pten^{-/-}; Sav1^{-/-}; Yap^{-/-}; Taz^{-/-}$ livers develop pronounced fibrosis.

(A) Schematic for the generation of $Pten^{-/-}; Sav1^{-/-}; Yap^{-/-}; Taz^{-/-}$ mice. (B-D) Liver-to-body weight ratio (B), Sirius red and CK19 immunohistochemical staining of the liver (C), and isolated serum color (D) for 1-month-old mice (n = 3) of the indicated genotypes. Scale bars (C), 200 μ m (top) or 100 μ m (bottom); arrows indicate ducts.

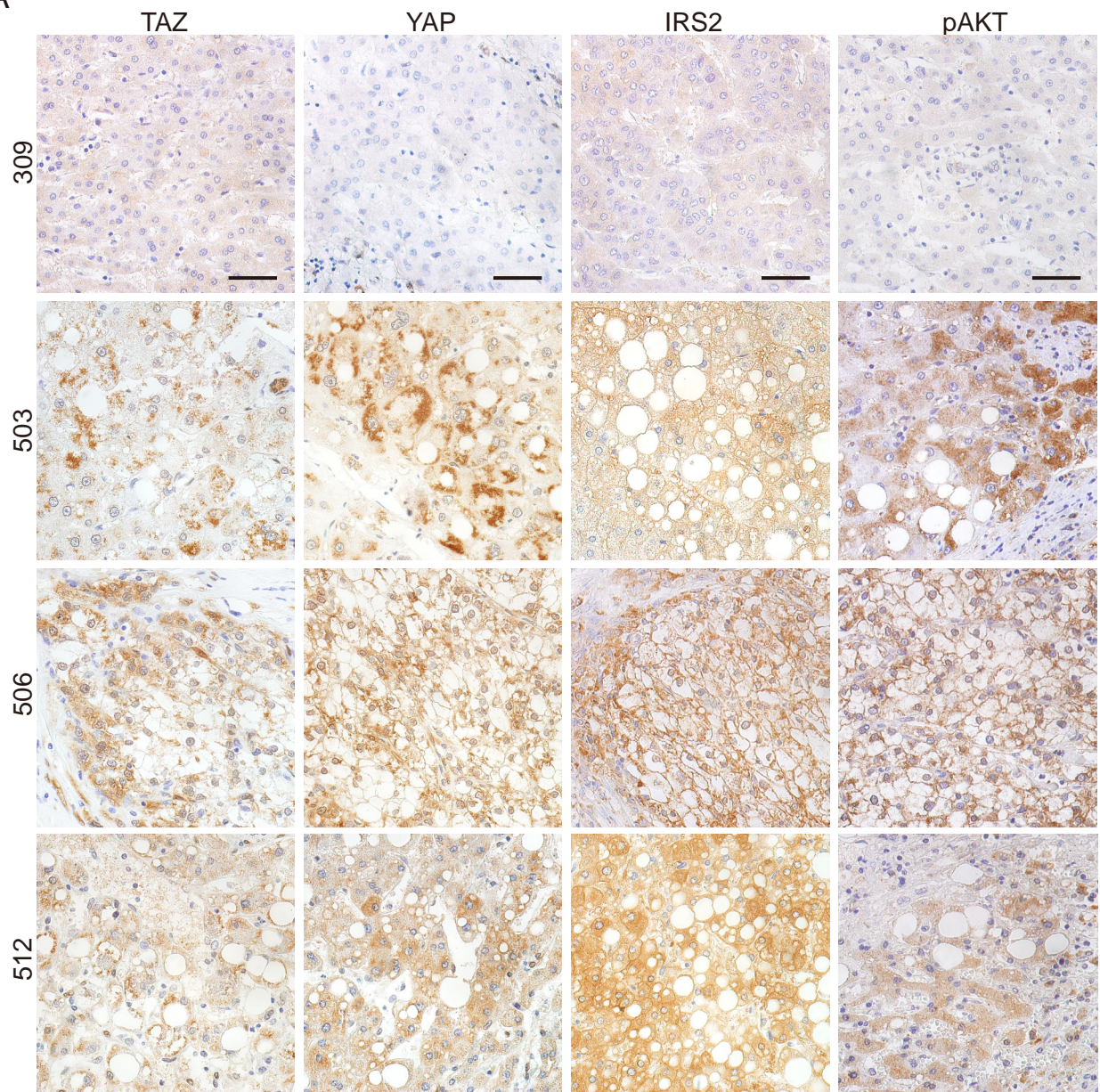


Supplemental Figure 4. The ablation of both *Yap* and *Taz* leads to ductal malformation and severe fibrosis. (A-G) Macroscopic appearance of the liver (A), isolated serum color (B), liver-to-body weight ratio (C), serum analysis (D, E), H&E, Sirius red, and CK19 immunohistochemical staining of the liver (F), and immunoblot analysis of the liver (G) for 1-month-old WT or liver-specific *Yap*^{-/-};*Taz*^{-/-} mice (each group, n = 3). Scale bars (F), 100 μ m (top and bottom) or 200 μ m (middle); arrows indicate ducts. T.Bilirubin, total bilirubin; Chol, cholesterol; TG, triglycerides. All quantitative data are means \pm s.e.m. **P* < 0.05, ***P* < 0.01, ****P* < 0.001 versus the corresponding WT value (Student's t test).



Supplemental Figure 5. Expression of a kinase-dead form of MST1 does not rescue the fatty liver phenotype of *Pten*^{-/-} mice. (A) Schematic for the generation of *Pten*^{-/-};MSTwt^{Tg} or *Pten*^{-/-};MSTkd^{Tg} mice. (B) Liver-to-body weight ratio for 2-month-old mice (each group, n = 3) of the indicated genotypes. Data are means ± s.e.m. (C-D) Macroscopic appearance (C), and immunoblot analysis (D) of the livers from 2-month-old mice (n = 3) of the indicated genotypes.

A



B

| Sample Number | Sex | Age | TAZ | YAP | IRS2 | pAKT |
|---------------|-----|-----|-----|-----|------|------|
| 501 | M | 78 | +++ | + | ++ | +++ |
| 503 | M | 83 | +++ | +++ | ++ | +++ |
| 504 | F | 58 | +++ | ++ | +++ | +++ |
| 506 | M | 76 | +++ | +++ | +++ | +++ |
| 507 | M | 62 | ++ | ++ | +++ | +++ |
| 509 | F | 72 | ++ | + | ++ | +++ |
| 510 | M | 75 | ++ | +++ | ++ | + |
| 512 | F | 69 | +++ | ++ | +++ | +++ |
| 515 | M | 72 | +++ | ++ | +++ | + |

C

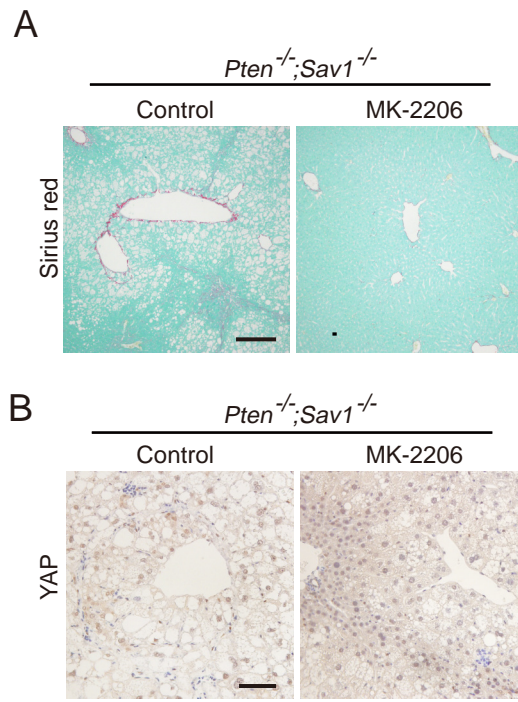
| | non-NAFLD | NAFLD | | non-NAFLD | NAFLD |
|------------|-----------|-------|-------------|-----------|-------|
| TAZ (Low) | 31 | 0 | IRS2 (Low) | 34 | 0 |
| TAZ (High) | 10 | 15 | IRS2 (High) | 7 | 15 |
| total | 41 | 15 | total | 41 | 15 |

| | non-NAFLD | NAFLD | | non-NAFLD | NAFLD |
|------------|-----------|-------|-------------|-----------|-------|
| YAP (Low) | 31 | 3 | pAKT (Low) | 37 | 6 |
| YAP (High) | 10 | 12 | pAKT (High) | 4 | 9 |
| total | 41 | 15 | total | 41 | 15 |

Supplemental Figure 6. Comparison of IHC intensities of TAZ, YAP, IRS2, and pAKT(S473) protein levels between NAFLD-associated HCC and non-NAFLD HCC.

(A) Representative immunohistochemical staining of TAZ, YAP, IRS2, and pAKT(S473) in human HCC not associated with NAFLD (sample No. 309) or associated with NAFLD (sample No. 503, 506, 512). Scale bars, 50 μ m. (B) Immunohistochemistry signal intensity scores for TAZ, YAP, IRS2, and pAKT in human HCC associated with NAFLD. -, no expression; +, low expression; ++, moderate expression; +++, high expression.

(C) The number of specimens with intense staining of TAZ, YAP, IRS2, and pAKT in the human HCC associated with NAFLD compared to HCC not associated with NAFLD (all $P < 0.001$, by chi-square test).



Supplemental Figure 7. Effects of MK-2206 treatment on the liver of DKO

mice. (A) Representative Sirius red staining of the liver of DKO mice treated for 2 weeks with MK-2206 or vehicle beginning at 3 weeks of age. Scale bar, 200 μ m. (B) Representative YAP staining of the liver of DKO mice treated for 2 weeks with MK-2206 or vehicle beginning at 12 weeks of age. Scale bar, 100 μ m.

Supplementary Table 1 Primer sequences for RT-qPCR analysis, luciferase reporter construction, ChIP-qPCR analysis, and mouse genotyping.

| RT-qPCR | | |
|----------------|--------------------------------|---------------------------------|
| Gene | Sense | Antisense |
| <i>Srebp1a</i> | 5'-GGCCGAGATGTGCGAACT-3' | 5'-TTGTTGATGAGCTGGAGCATGT-3' |
| <i>Srebp1c</i> | 5'-GGAGCCATGGATTGCACATT-3' | 5'-CAGGAAGGCTTCCAGAGAGG-3' |
| <i>Srebp2</i> | 5'-GCGTTCTGGAGACCATGGA-3' | 5'-ACAAAGTTGCTCTGAAAACAAATCA-3' |
| <i>Fasn</i> | 5'-GCCTACACCCAGAGCTACCG-3' | 5'-GCCATGGTACTTGGCCTTG-3' |
| <i>Acc1</i> | 5'-CAACGAGATTTCACTGTGGCT-3' | 5'-TTCTGCATTGGCTTTAAGGTCT-3' |
| <i>Scd1</i> | 5'-CCGAGACCCCTTAGATCGA-3' | 5'-TAGCCTGTAAAGATTTCTGCAAACC-3' |
| <i>Tnfa</i> | 5'-CATCTTCTCAAAATTCGAGT-3' | 5'-TGGGAGTGACAAGGTACAA-3' |
| <i>Il6</i> | 5'-TCCACGATTCCCAGAGAAC-3' | 5'-AGTTGCCTTCTTGGGACTGA-3' |
| <i>Irs2</i> | 5'-CAAGAGCCCTGGCGAGTACA-3' | 5'-CCGCGGATGCCAGTAGTG-3' |
| <i>Acta2</i> | 5'-ATGCTCCCAGGGCTGTTTTCCCAT-3' | 5'-GTGGTGCCAGATCTTTTCCATGTCG-3' |
| <i>Desmin</i> | 5'-CTAAAGGATGAGATGGCCCG-3' | 5'-GAAGGTCTGGATAGGAAGGTTG-3' |
| <i>Tgfb</i> | 5'-CTCCCGTGGCTTCTAGTGC-3' | 5'-GCCTTAGTTTGGACAGGATCTG-3' |
| <i>Hmox1</i> | 5'-GCTCGAATGAACACTCTGG-3' | 5'-GTTCTCTGTCAGCATCAC-3' |
| <i>Gadd153</i> | 5'-CTGGAAGCCTGGTATGAGGAT-3' | 5'-CAGGGTCAAGAGTAGTGAAGGT-3' |

| Luciferase reporter construction | | |
|----------------------------------|----------------------------------|--------------------------------|
| Region | Sense | Antisense |
| TBS1 | 5'-CTTATCTGGCAGCAGGAAGGAGAG-3' | 5'-CACACCCTCGCACACATATCCCTC-3' |
| TBS2 | 5'- CACCCTTGACACACGTAGAGACGCT-3' | 5'- ACCGTGTTACCCAGCACCAGGGG-3' |
| TBS3 | 5'-CCTGGCAGTGTCCTATAGTTGA -3' | 5'- CAGCTGCTGCTTCTTTAGGGG-3' |
| TBS4 | 5'- GCAGCAGCTGAAGTGCTAAAGA-3' | 5'-GCTGCTTTCCTCTCATTGCTC -3' |
| TBS5 | 5'- GCCTCTGAGCCAACATCTCT-3' | 5'-TATGACCTCCCACCCACTTCA -3' |
| TBS6 | 5'- CATGGCTCGTTTCTCCTTCTGG-3' | 5'-GAGTACTCAGGCCAGGATGC -3' |

| ChIP-qPCR | | |
|-----------|---------------------------------|----------------------------------|
| Region | Sense | Antisense |
| TBS1 | 5'-ATCTATGGTCTTCAGAATCACAC-3' | 5'-CCAGAGTTTATCTTACAATTTAACCT-3' |
| TBS2 | 5'-CACAGTTTACACAAAGGGTAAAGCA-3' | 5'-GCTCTGGATGCGTAAACAAAACA-3' |
| TBS4 | 5'-GCAGCAGTTGATTCCCATCCT-3' | 5'-ACAATGGGGCAGGGAAGGTA-3' |
| TBS5 | 5'-GTAAAACCCAGAAACCCCACTTTC-3' | 5'-TGCTCTGCTTCTCTCACTAGGA-3' |

Mouse genotyping

| Gene | Sense | Antisense |
|-------------------------|--|---------------------------------------|
| <i>Sav1</i> | 5'-TGGTTTGCTTTTATAGTGCC-3' | 5'-TGCTGGTTTTGTCTCACTAA-3' |
| <i>Pten</i> | 5'-CTC CTC TAC TCC ATT CTT CCC-3' | 5'-ACT CCC ACC AAT GAA CAA AC-3' |
| <i>Yap1</i> | 5'-ACATGTAGGTCTGCATGCCAGAGGAGG-3' | 5'-AGGCTGAGACAGGAGGATCTCTGTGAG-3' |
| <i>Taz</i> | 5'-GGCTTGTGACAAAGAACCTGGGGCTATCTGAG-3' | 5'-CCCACAGTTAAATGCTTCTCCCAAGACTGGG-3' |
| <i>Cre</i> | 5'-GTGTTGCCGCGCCATCTGC-3' | 5'-CACCATTGCCCTGTTTCACTATC-3' |
| <i>MST^{Tg}</i> | 5'-GCTCTAGAGCCTCTGCTAACCA-3' | 5'-CCAGGGACCAGATGTCTGC-3' |

AAV-sgIrs2

| Region | Sense | Antisense |
|--------------|-----------------------------------|----------------------------------|
| <i>Ex1-1</i> | 5'- CACC GATCGCCCTCTACACCAAGG-3' | 5'- AAAC CCTTGGTGTAGAGGGCGATC-3' |
| <i>Ex1-2</i> | 5'- CACC GCCGCCGCGAGCCTCCGCGGC-3' | 5'- AAAC GCCGCGGAGGCTGCGGCGGC-3' |

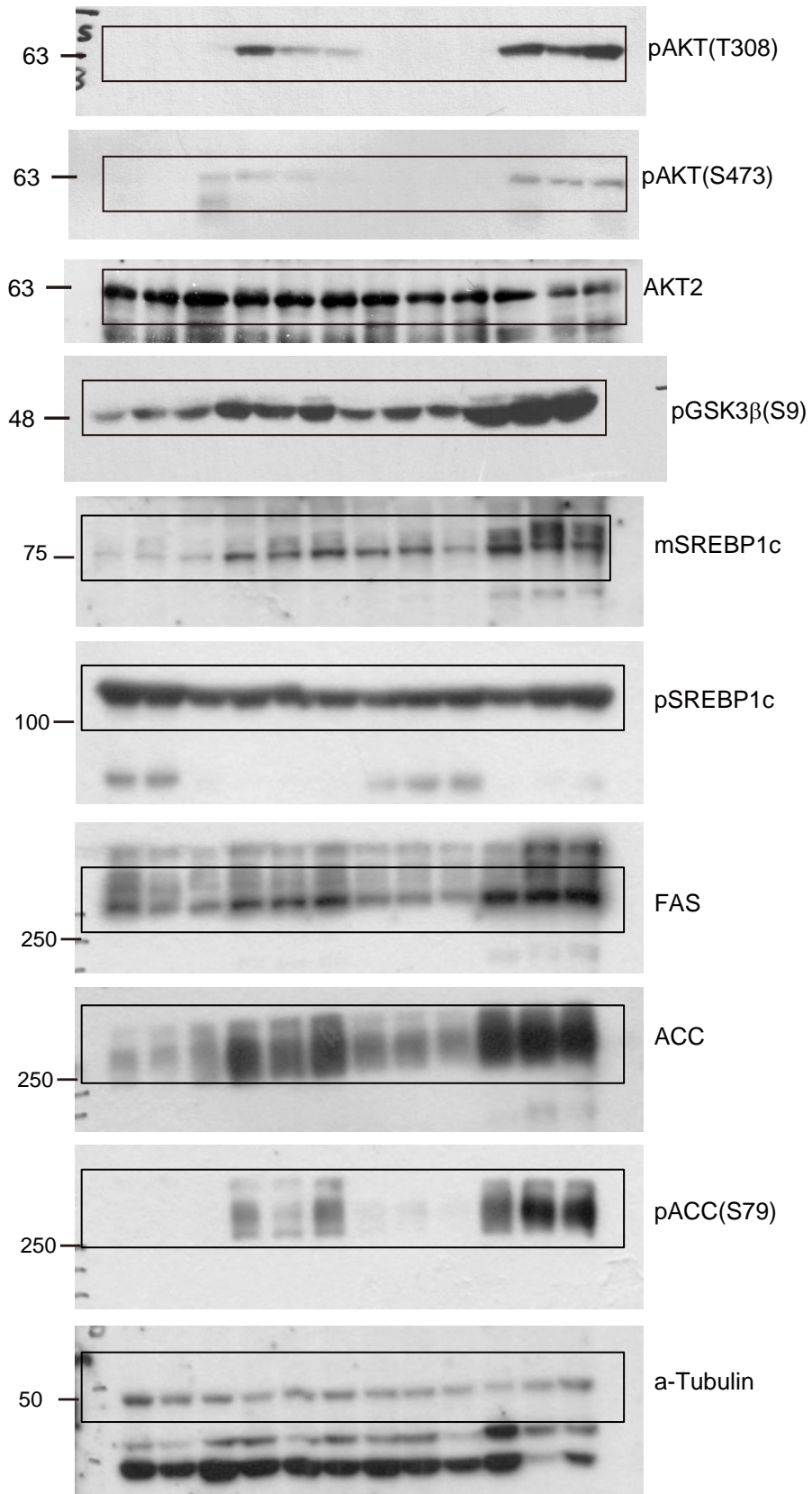
Full unedited blot

The Hippo-YAP/TAZ Pathway Suppresses IRS2-AKT Signaling to Prevent Fatty Liver and Liver Cancer

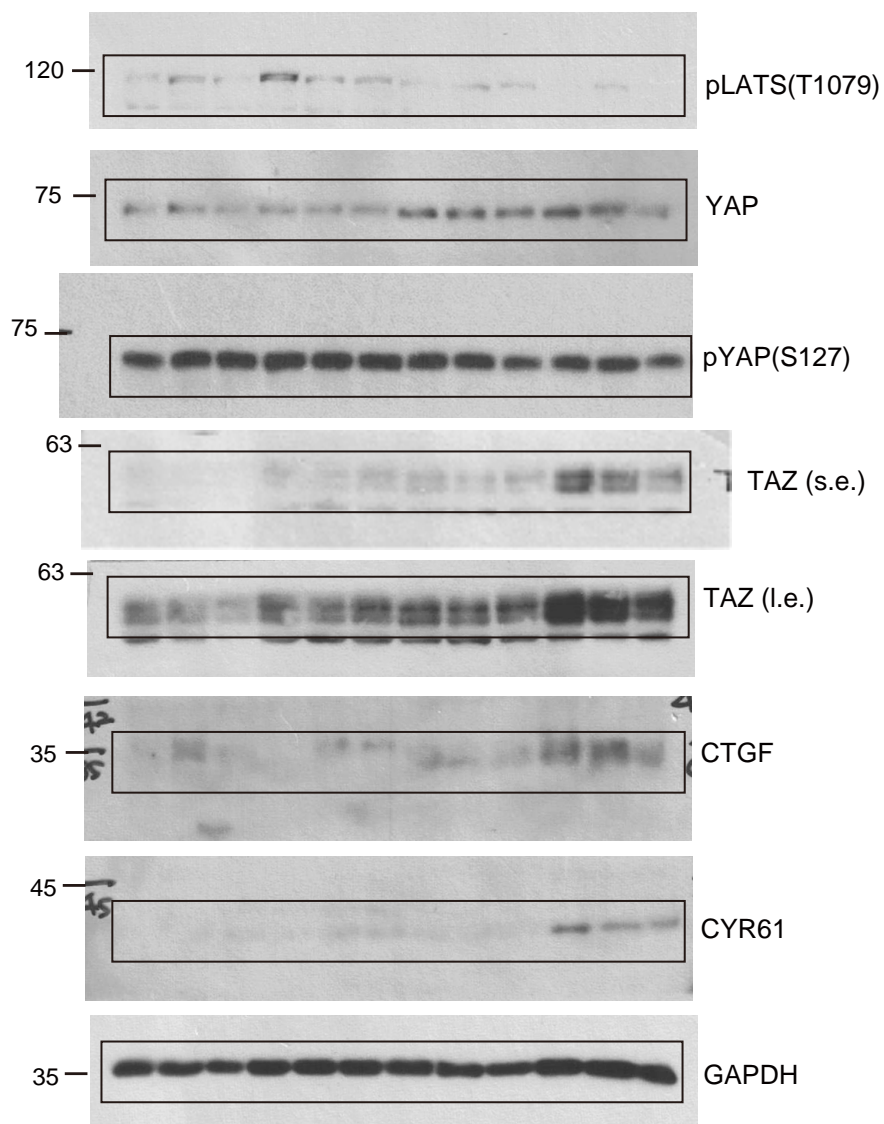
It includes;

1. Full unedited blot for Figure 2D, 3A, 3D, 3G, 3H, 4A, 4C, 4D, 4E, 4F, 4G, 5B, 5F and 7M.
2. Full unedited blot for Supplemental Figure 4G and 5D.

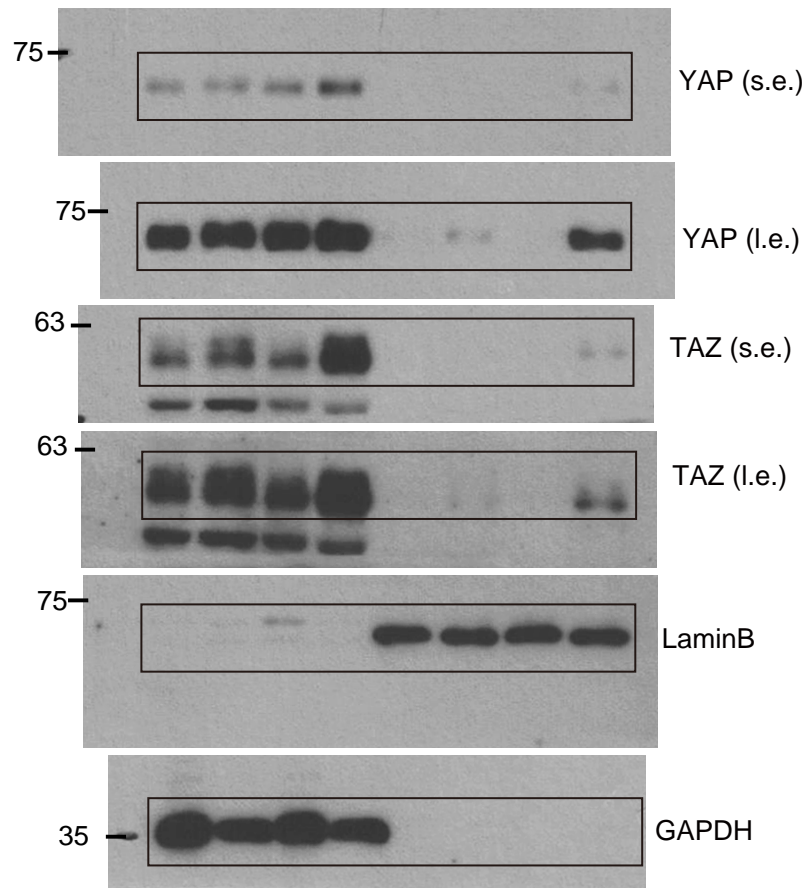
Full unedited blot for Figure 2D



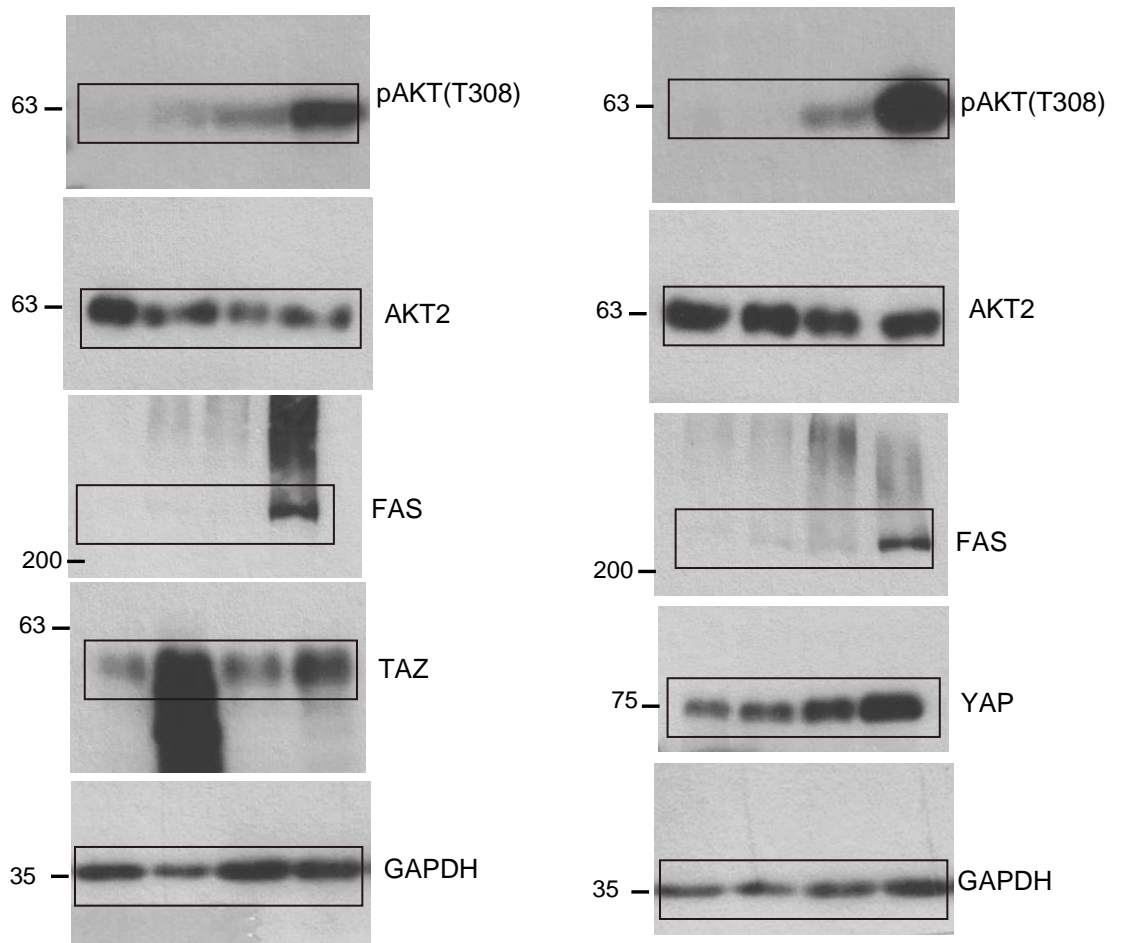
Full unedited blot for Figure 3A



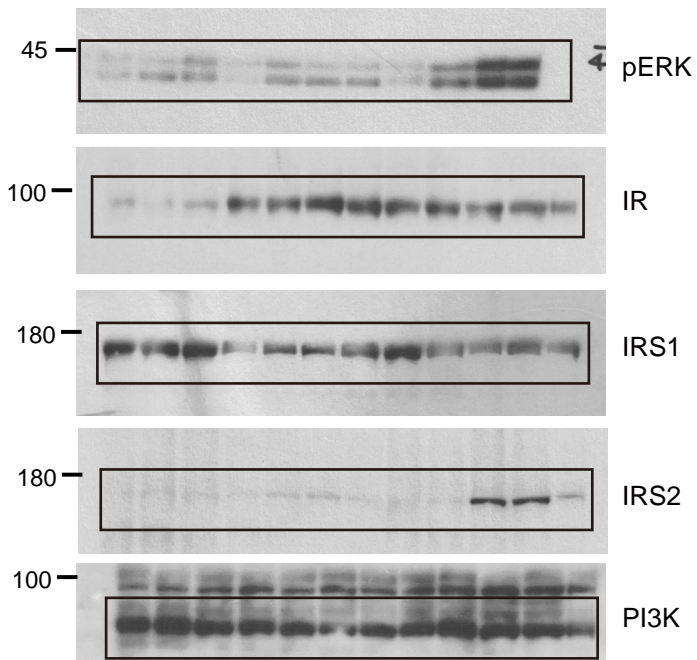
Full unedited blot for Figure 3D



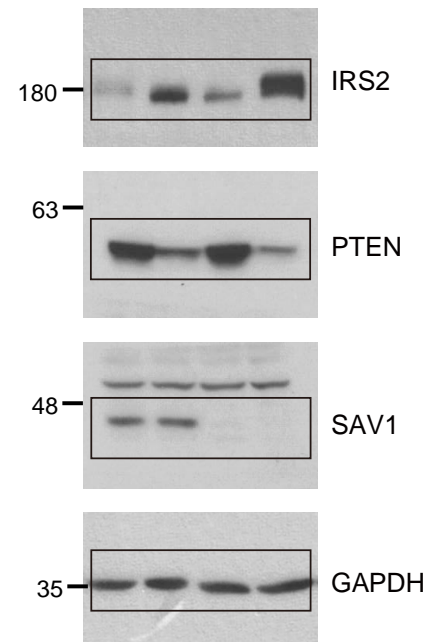
Full unedited blot for Figure 3G, H



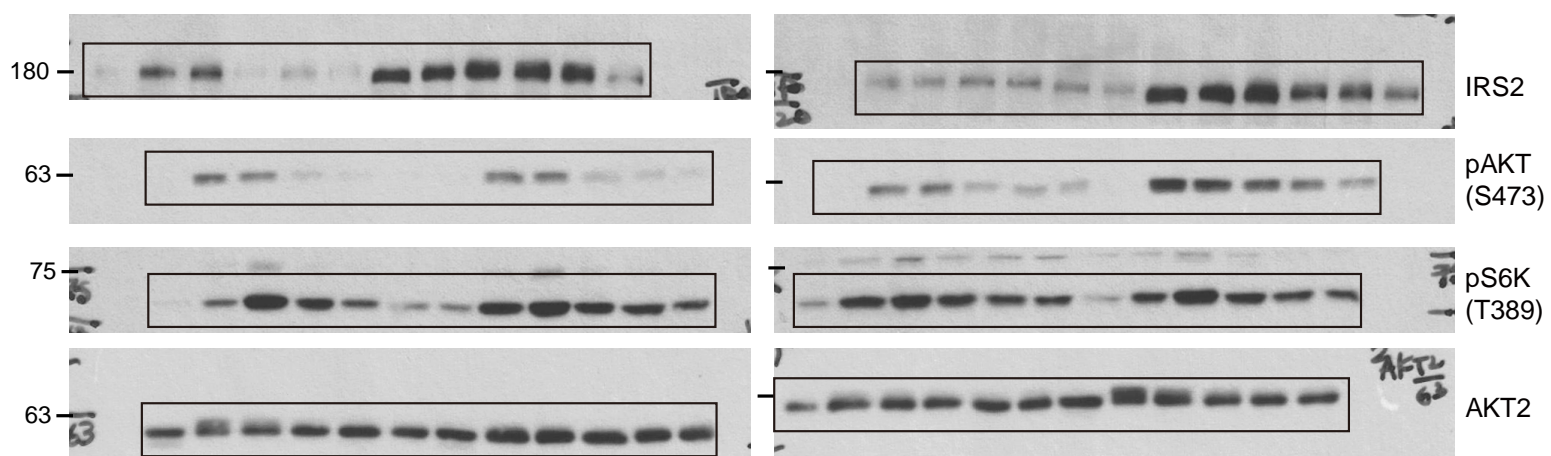
Full unedited blot for Figure 4A

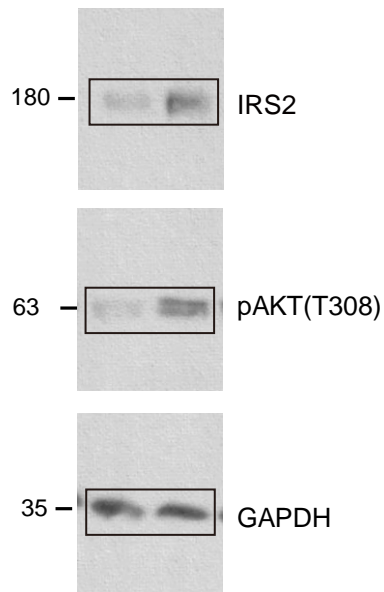
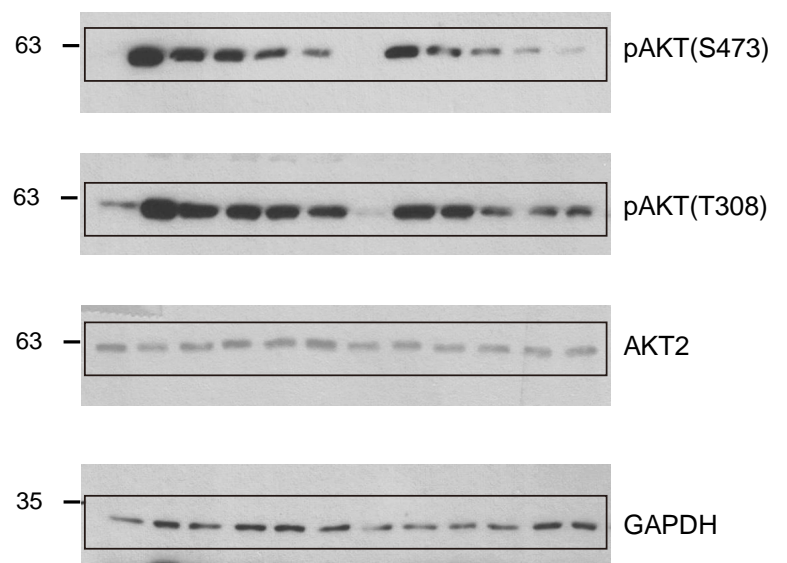
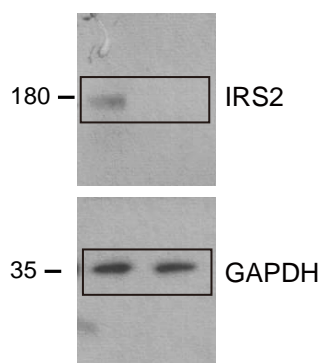
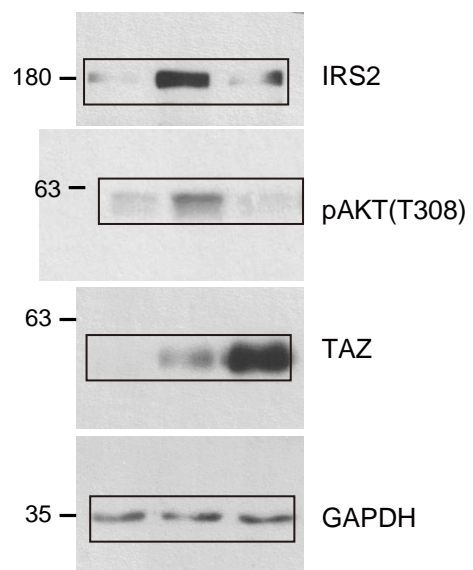


Full unedited blot for Figure 4C

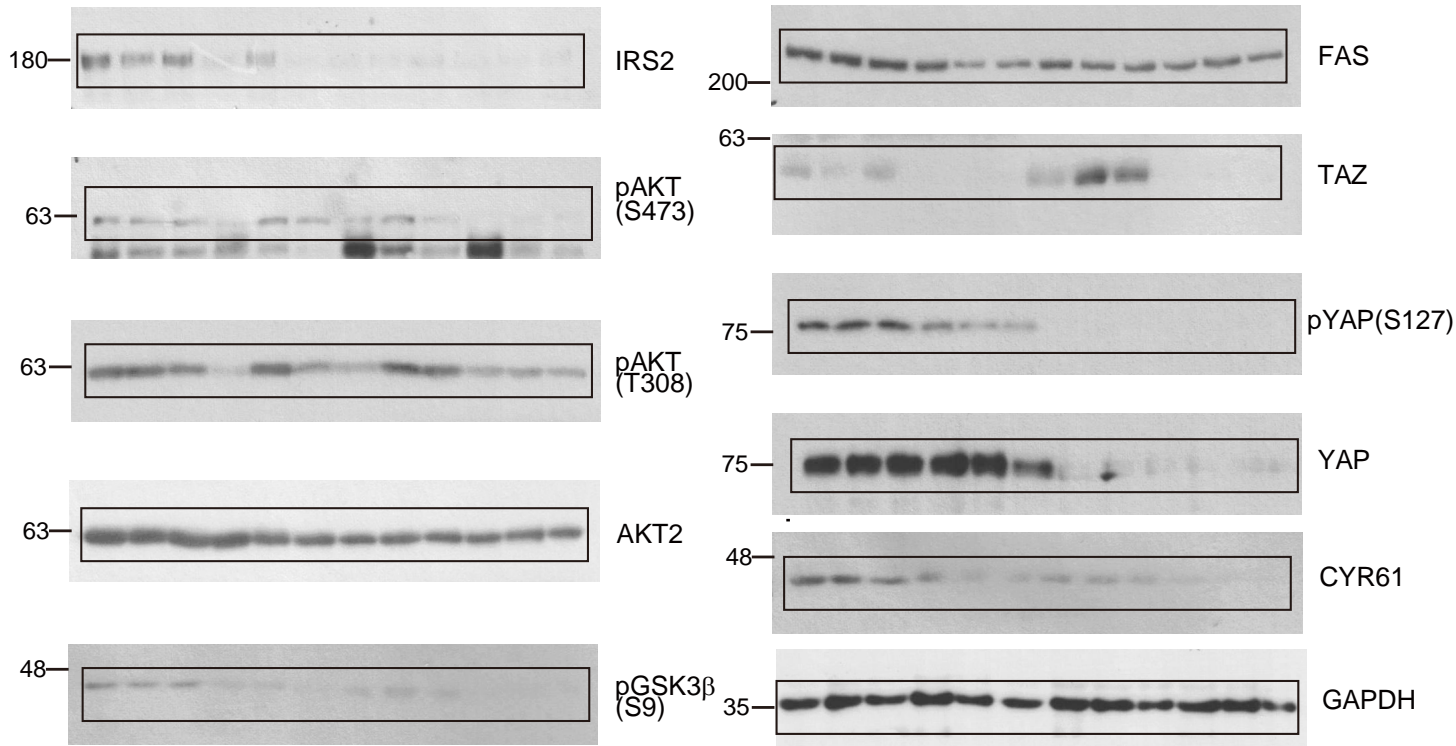


Full unedited blot for Figure 4D

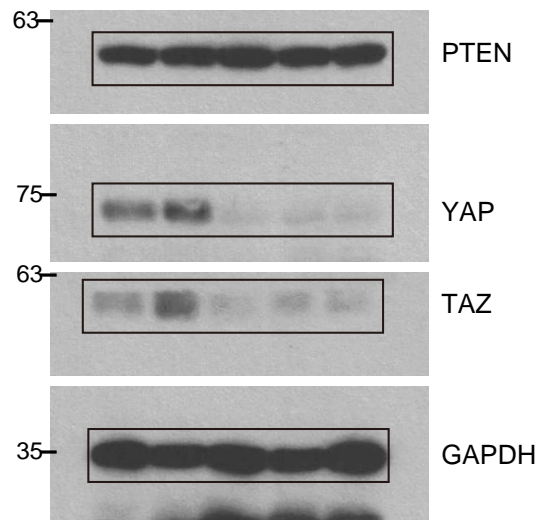


Full unedited blot for Figure 4EFull unedited blot for Figure 4FFull unedited blot for Figure 4FFull unedited blot for Figure 4G

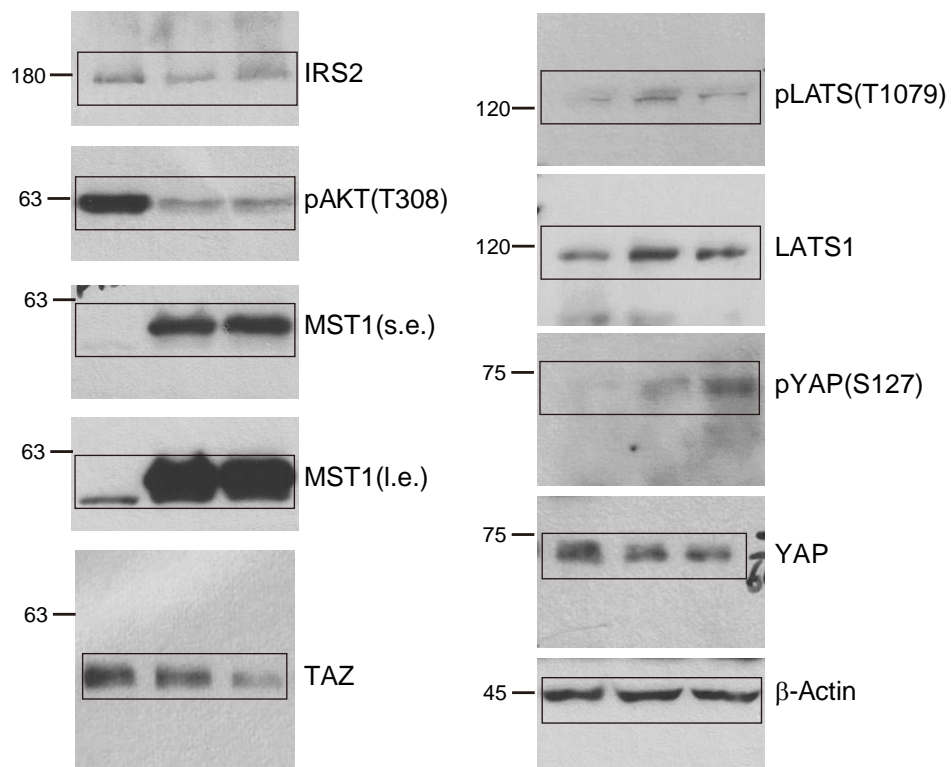
Full unedited blot for Figure 5B



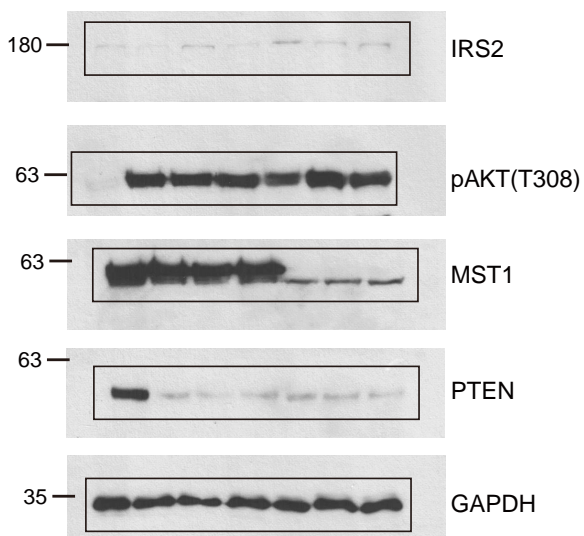
Full unedited blot for Figure S4G



Full unedited blot for Figure 5F



Full unedited blot for Figure S5D



Full unedited blot for Figure 7M

